AFRL-AFOSR-VA-TR-2015-0295

EXPERIMENTAL INVESTIGATION OF TURBULENT FLAMES IN HYPERSONIC FLOWS

Hyungrok Do
UNIVERSITY OF NOTRE DAME DU LAC

09/01/2015
Final Report

Air Force Research Laboratory
AF Office Of Scientific Research (AFOSR)/ RTA1
Arlington, Virginia 22203
Air Force Materiel Command

REPORT DOCUMENTATION PAGE

Form Approved
OMB No. 0704-0188

PLEASE DO NOT RETURN YOUR FORM TO THE ABOVE ORGANIZATION.

1. REPORT DATE *(DD-MM-YYYY)*	2. REPORT TYPE	3. DATES COVERED *(From - To)*
31-08-2015	Final Report	04/01/2012 - 06/30/2015

4. TITLE AND SUBTITLE
Experimental Investigation of Turbulent Flames in Hypersonic Flows

5a. CONTRACT NUMBER

5b. GRANT NUMBER
FA9550-12-1-0161

5c. PROGRAM ELEMENT NUMBER

6. AUTHOR(S)
Hyungrok Do

5d. PROJECT NUMBER

5e. TASK NUMBER

5f. WORK UNIT NUMBER

7. PERFORMING ORGANIZATION NAME(S) AND ADDRESS(ES)
University of Notre Dame
Notre Dame, Indiana

8. PERFORMING ORGANIZATION REPORT NUMBER

9. SPONSORING/MONITORING AGENCY NAME(S) AND ADDRESS(ES)
Air Force Office of Scientific Research
875 North Randolph Street
Suite 325, Room 3112
Arlington VA, 22203

10. SPONSOR/MONITOR'S ACRONYM(S)
AFOSR

11. SPONSOR/MONITOR'S REPORT NUMBER(S)

12. DISTRIBUTION/AVAILABILITY STATEM
Distribution A

13. SUPPLEMENTARY NOTES

14. ABSTRACT
Work during the three-year project timeframe has been focused on 1-1) completing the construction of an arc-heated hypersonic combustion test rig (ACT-1) at the University of Notre Dame (ND), 1-2) characterizing turbulent flame dynamics under various supersonic and hypersonic freestream conditions (Mach 4.5, 6 and 9), and 1-3) developing tools for quantitative turbulent flow measurement methods (in collaboration with Dr. Campbell D. Carter of AFRL) including a new laser diagnostics technique for simultaneous fuel concentration and gas density measurements in supersonic combustors, and 1-4) controlling/quantifying freestream turbulence and evaluating its influences on the turbulent flame dynamics in the high-Reynolds scramjet flows.

15. SUBJECT TERMS

16. SECURITY CLASSIFICATION OF:			17. LIMITATION OF ABSTRACT	18. NUMBER OF PAGES	19a. NAME OF RESPONSIBLE PERSON
a. REPORT	b. ABSTRACT	c. THIS PAGE			Hyungrok Do
U	U	U	SAR		19b. TELEPHONE NUMBER *(Include area code)* 574-631-1189

Reset

INSTRUCTIONS FOR COMPLETING SF 298

1. REPORT DATE. Full publication date, including day, month, if available. Must cite at least the year and be Year 2000 compliant, e.g. 30-06-1998; xx-06-1998; xx-xx-1998.

2. REPORT TYPE. State the type of report, such as final, technical, interim, memorandum, master's thesis, progress, quarterly, research, special, group study, etc.

3. DATES COVERED. Indicate the time during which the work was performed and the report was written, e.g., Jun 1997 - Jun 1998; 1-10 Jun 1996; May - Nov 1998; Nov 1998.

4. TITLE. Enter title and subtitle with volume number and part number, if applicable. On classified documents, enter the title classification in parentheses.

5a. CONTRACT NUMBER. Enter all contract numbers as they appear in the report, e.g. F33615-86-C-5169.

5b. GRANT NUMBER. Enter all grant numbers as they appear in the report, e.g. AFOSR-82-1234.

5c. PROGRAM ELEMENT NUMBER. Enter all program element numbers as they appear in the report, e.g. 61101A.

5d. PROJECT NUMBER. Enter all project numbers as they appear in the report, e.g. 1F665702D1257; ILIR.

5e. TASK NUMBER. Enter all task numbers as they appear in the report, e.g. 05; RF0330201; T4112.

5f. WORK UNIT NUMBER. Enter all work unit numbers as they appear in the report, e.g. 001; AFAPL30480105.

6. AUTHOR(S). Enter name(s) of person(s) responsible for writing the report, performing the research, or credited with the content of the report. The form of entry is the last name, first name, middle initial, and additional qualifiers separated by commas, e.g. Smith, Richard, J, Jr.

7. PERFORMING ORGANIZATION NAME(S) AND ADDRESS(ES). Self-explanatory.

8. PERFORMING ORGANIZATION REPORT NUMBER. Enter all unique alphanumeric report numbers assigned by the performing organization, e.g. BRL-1234; AFWL-TR-85-4017-Vol-21-PT-2.

9. SPONSORING/MONITORING AGENCY NAME(S) AND ADDRESS(ES). Enter the name and address of the organization(s) financially responsible for and monitoring the work.

10. SPONSOR/MONITOR'S ACRONYM(S). Enter, if available, e.g. BRL, ARDEC, NADC.

11. SPONSOR/MONITOR'S REPORT NUMBER(S). Enter report number as assigned by the sponsoring/ monitoring agency, if available, e.g. BRL-TR-829; -215.

12. DISTRIBUTION/AVAILABILITY STATEMENT. Use agency-mandated availability statements to indicate the public availability or distribution limitations of the report. If additional limitations/ restrictions or special markings are indicated, follow agency authorization procedures, e.g. RD/FRD, PROPIN, ITAR, etc. Include copyright information.

13. SUPPLEMENTARY NOTES. Enter information not included elsewhere such as: prepared in cooperation with; translation of; report supersedes; old edition number, etc.

14. ABSTRACT. A brief (approximately 200 words) factual summary of the most significant information.

15. SUBJECT TERMS. Key words or phrases identifying major concepts in the report.

16. SECURITY CLASSIFICATION. Enter security classification in accordance with security classification regulations, e.g. U, C, S, etc. If this form contains classified information, stamp classification level on the top and bottom of this page.

17. LIMITATION OF ABSTRACT. This block must be completed to assign a distribution limitation to the abstract. Enter UU (Unclassified Unlimited) or SAR (Same as Report). An entry in this block is necessary if the abstract is to be limited.

FINAL REPORT

EXPERIMENTAL INVESTIGATION OF TURBULENT FLAMES IN HYPERSONIC FLOWS (FA9550-12-1-0161)

AUG 2015, PI: Hyungrok Do

Assistant Professor, Department of Aerospace and Mechanical Engineering, University of Notre Dame, Notre Dame, IN, 46556

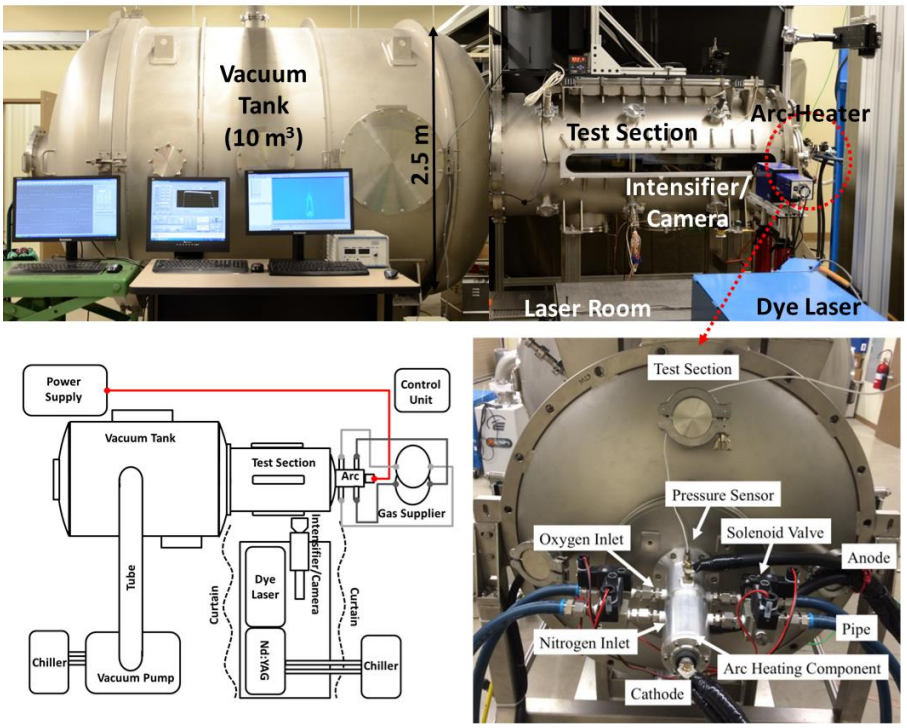

Figure 1. Pictures and a schematic (bottom left) of the arc-heated hypersonic wind tunnel (ACT-1) built at University of Notre Dame (ND).

Work during the three-year project timeframe has been focused on **1-1)** completing the ***construction of an arc-heated hypersonic combustion test rig (ACT-1)*** at the University of Notre Dame (ND), **1-2)** characterizing ***turbulent flame dynamics*** under various supersonic and hypersonic freestream conditions (Mach 4.5, 6 and 9), and **1-3)** developing tools for quantitative turbulent flow measurement methods (in collaboration with Dr. Campbell D. Carter of AFRL) including a new laser diagnostics technique for ***simultaneous fuel concentration and gas density measurements in supersonic combustors,*** and **1-4)** ***controlling/quantifying freestream turbulence and evaluating its influences on the turbulent flame dynamics in the high-Reynolds scramjet flows***. The new arc-heated hypersonic facility (Fig. 1) construction was completed at ND in the second project year, which has been fully operational afterwards

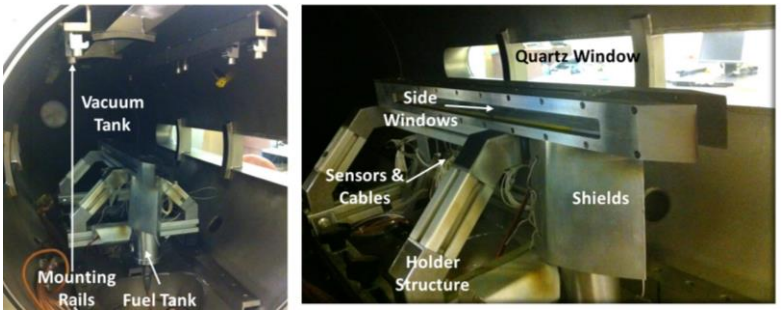

Figure 2. A scramjet test model inside the test section of the ACT-1.

for the supersonic/hypersonic turbulent combustion study. The studies on the supersonic flame dynamics were successfully conducted revealing non-premixed/partially-premixed characteristics of the ethylene flames in the model scramjet installed in the hypersonic facility (Fig. 2). The experimental results also confirmed the critical effects of the freestream turbulence on the flame dynamics both for partially- and non-premixed configurations. In addition, a new laser diagnostics tool specialized for the high-enthalpy scramjet study has been developed and used in collaboration with AFRL at Wright Patterson Air Force Base. This technique was proven to be working perfectly under the harsh flow conditions of high-speed (Ma > 4.5) and high-temperature (> 1,500K) that limit quantitative measurements.

Facilitated by the **1-1) completion of ACT-1 construction** and **1-3) developments of the new optical measurement tools**, **1-2)** ***we have investigated fundamental turbulent premixed and non-premixed combustion dynamics*** **1-4)** ***interacting with the high-Reynolds flows and being dominated by high-frequency and small-scale turbulence.*** The turbulence directly and indirectly influences non-/partially-premixed combustion chemistry by transporting combustion products including heat (thermal energy) and new/pre-existing species from/to the combustion zone. To understand this fundamental science of the complex physiochemical phenomena occurring in the high-Reynolds environments, the turbulence properties, particularly near the Kolmogorov limit, needs to be quantified at upstream and downstream of shockwaves/flames. More specifically, this is for understanding how turbulence structures (from Kolmogorov to integral scales) interact/influence/alter the critical rate-limiting process that is the partially-premixed-combustion chemistry in this study; the partially-premixed-combustion is the primary source of thermal energy producing the scramjet thrust. The shockwaves and flames significantly affect fluid/flow properties to alter turbulence properties that again influences premixed combustion chemistry. Nevertheless, in practice, we have limited access to these high-Reynolds phenomena due to the limited quantitative experimental methods resolving the high-frequency turbulence behaviors in both the reacting/non-reacting flows. The new ACT-1 high-enthalpy facility was optimized for quantitative optical measurements and we have developed new quantitative optical methods of high-temporal/spatial resolutions that are essential for this study.

For enabling the extensive investigations on the turbulent combustion dynamics, turbulence in the test facility needs to be well-controlled, evenly-distributed (uniform) and well-characterized. In addition,

rapid fuel/air mixing upstream of the region of interest should be achieved to study partially-premixed turbulent combustion phenomena. Therefore, various tools for freestream turbulence control were tested, and influences of the freestream turbulence on scramjet flows first and then the complex turbulence combustion dynamics were systematically investigated. ***The overall combustion dynamics are resulting from the combination of non-premixed and partially-premixed flames interacting with the turbulence and the internal flow structures developing in the scramjet.*** Flow separations, corner flows, shock-boundary layer interactions, and boundary layer developments on the internal surfaces of the scramjet combustor are remarkable flow structures being altered by the freestream turbulence, which provide slow flow regions to aid flame stabilization. On the other hand, the turbulence itself also interacts directly with the non-premixed and partially-premixed flames appearing in scramjets. The non-premixed flame often attached on the fuel jet gets stronger and thicker with the increased turbulence when with sufficient freestream enthalpy igniting the jet flame. More importantly, the partially-premixed flames starting from far downstream region where the fuel and air are relatively well-mixed were significantly enhanced by the increased freestream turbulence under a fixed flow condition, e.g., with a fixed Mach number, pressure, and temperature.

Finally, the critical effect of the inlet design on the combustion dynamics was demonstrated via a set of experiments with varied scramjet inlet geometry (not presented in this report though). This is because the inlet geometry determines flow properties in scramjets that include turbulence intensity/spectrum, Mach number, pressure, and temperature.

This work has been performed by Dr. Hyungrok Do and a graduate student, Qili Liu under the guidance of Dr. Chiping Li.

1 Technical Synopsis

The following is a summary of the results obtained during the three-year project timeframe.

1-1) Arc-Heated Combustion Test Rig at ND (ACT-1)

ACT-1: A novel pulsed-arc-heating system (Figs. 1 and 2) is designed and built to provide high-enthalpy flows that expand through a converging/diverging (C/D) nozzle into a vacuum chamber accommodating the test section of the hypersonic facility (ACT-1). Two compressed gas supply tanks connected to the arc heater provide constant pressure gas flows through an arc and into a gas-mixing chamber downstream of the arc, respectively. The compressed nitrogen injected via two gas injection ports located upstream of the arc is heated in the arc region, mixed with oxygen in the mixing chamber downstream of the arc, and

expands through the C/D nozzle. Gas composition of the mixture escaping the arc-heating unit is controlled by gas pressures at the injection ports (e.g., two nitrogen and two oxygen ports). This new arc-heater configuration is designed mainly to minimize NOx production that affects flame dynamics (e.g., NOx reduces ignition delay). The new heater can prevent prompt NOx production in the arc region while thermal NOx production in the mixing chamber will still be significant. The thermal NOx production can be effectively minimized by reducing flow residence time in the chamber prior to the expansion into the vacuum chamber that lowers static mixture temperature rapidly. Multiple layers of the turbulent exciters are installed in the mixing chamber to facilitate gas mixing, however, estimated flow residence time (< 10 ms) in it is sufficiently short for significant reduction of thermal NOx production. Except for the new arc-heating unit built for this combustion study, the facility employs typical hypersonic facility design that has been utilized over the past 10 years, e.g., spatial pitot pressure distribution on the C/D nozzle exit plane is relatively uniform with random variations of maximum 5% of mean value. The arc heater is connected to a 260 kW DC power supply delivering current of 630 A to produce flows of up to 6 MJ/kg and 1 MPa at a stagnation condition. A settling chamber upstream of the C/D nozzle has a pressure sensor and an optical access window for emission spectroscopy to monitor the stagnant gas condition. The test condition is repeatable within 2 % variations in stagnation pressure and arc current/voltage.

The hypersonic wind tunnel facility implemented with the new pulsed-are-heater (Fig. 1) is used to generate Mach 4.5 – 9 flows of various freestream gas composition and total pressure/temperature. A clean core flow area in the test section of the facility is approximately 60 mm to 150 mm in diameter depending on C/D nozzle geometries, which is large enough to accommodate the model scramjet having 15 × 40 mm^2 cross section. The axisymmetric C/D nozzles produce gas flows at steady-state in the test section for a test time of one-second. The stagnation temperature (T_0) of the freestream flow is varied from 1,500 K to 3,500 K, which is a flow enthalpy range for auto-ignition (> 1,500 K) of partially-premixed flames downstream of the fuel jet without significant non-premixed flames on fuel jets. Fuel concentration that is controlled by fuel jet injection pressure (flow rate) is varied in a wide range in terms of overall equivalence ratio, (ϕ) = 0.2 – 5.5, in the model scramjet. The overall equivalence ratio is derived assuming that the injected fuel is perfectly mixed with the freestream flow captured by the inlet of the model scramjet.

Model Scramjet: A model scramjet (Fig. 3) installed in the hypersonic wind tunnel is made of stainless steel, which is 600 mm in length with an internal flow channel of 15 mm (height) × 40 mm (width) rectangular constant cross section. The inlet of the model consists of sharp leading edges; bottom and side lips are wedged outside and flat on internal surfaces to minimize shock induction into the internal flow channel (scramjet inlet/isolator/combustor). The angle of the inlet upper lip on the internal surface is 6° or 12° (interchangeable) to produce an incident shockwave into the model scramjet; both the inlets (6° or

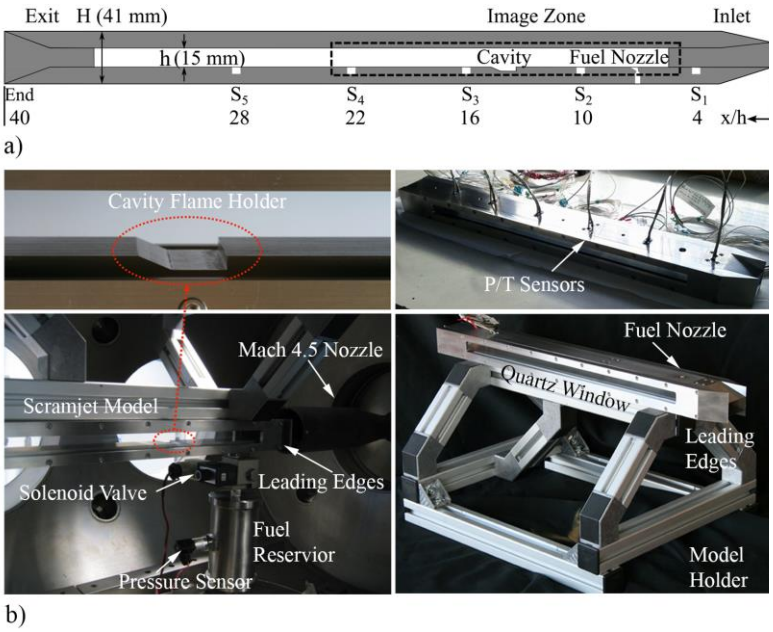

Figure 3. a) A schematic and b) pictures of the model scramjet installed in the test section of the hypersonic facility.

12°) have the same flow capture area (entrance height of inlet 19.3 mm). An oblique supersonic jet of 1.6 mm in diameter at the throat expands through a diverging section of 22.5° divergent angle and 60° inclination toward downstream, which is located 100 mm downstream from the inlet lip on the centerline of the bottom wall (the isolator (constant cross sectional area) length is approximately 80 mm with 12° inlet upper lip angle). The exit of fuel jet nozzle on the scramjet surface is an ellipse, 5.9 mm by 5.0 mm. The expanding supersonic fuel jet is to extend the jet sweep area for facilitating fuel/oxidizer mixing and, possibly, to avoid non-premixed flame ignition on the windward side of the jet by increasing stretch rate on the jet. As shown in Fig. 2 (bottom left), a solenoid valve controlling ethylene injection and a fuel reservoir maintaining constant fuel pressure during the jet injection period are connected to the fuel jet nozzle. The fuel pressure traces are recorded by a pressure sensor attached on the reservoir. Overall fuel equivalence ratio (ϕ) in the combustor is estimated by the ratio of ethylene jet mass flow rate and freestream flow rate through the model scramjet. A wall cavity is located at 100 mm downstream from the jet nozzle (i.e., 200 mm downstream from the inlet lip) in the bottom wall of the scramjet model, with the dimensions of 3 mm in depth, 12 mm in length along the freestream flow direction and 22.5° ramp (back step) angle. Five pressure sensors (Kulite) and five temperature sensors (MEDTHERM coaxial thermocouple, type K) are mounted in the bottom wall, (S 1 through 5 in Fig. 3a) to record surface pressure/temperature traces.

1-2) Turbulent Ethylene Flame Dynamics in a Model Scramjet

Ethylene Flame Ignition and Stabilization: Three ethylene flame ignition (auto ignition) locations in the model scramjet are identified, which are in ***i) a partially-premixed region downstream of the cavity where fuel and air are relatively well mixed, ii) a cavity flameholder machined 100 mm downstream from the fuel jet, and iii) on the windward side of the ethylene fuel jet***. The ethylene flame first appears

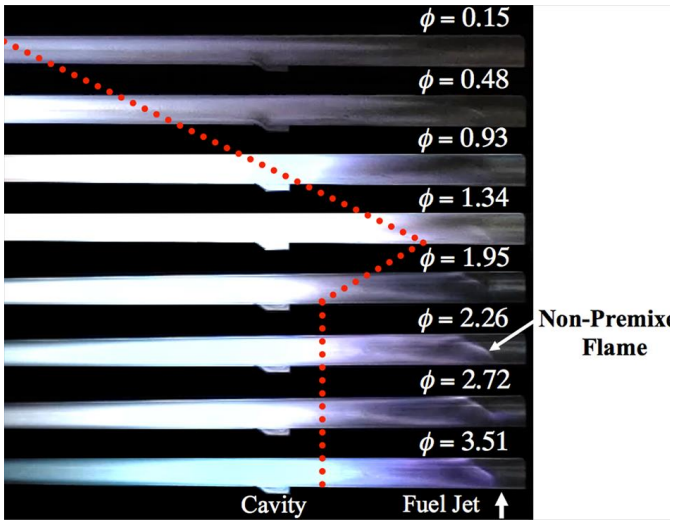

Figure 4. Quasi-stable ethylene flames with a Mach 4.5 freestream of T_0 = 2,500 K, P_0 = 100 kPa and ϕ = 0.15 – 3.51 (6° upper lip angle). Red dotted lines indicate locations of the partially-premixed quasi-stable flames.

at one or two of the three ignition locations depending on flow conditions such as overall fuel concentration and flow enthalpy. The flame auto ignition is observed with Mach 4.5, 6 and 9 flows of high enthalpy above 1,800 K stagnation temperature.

Flame ignition at a location downstream of the cavity (partially-premixed zone) is observed in most of the flow conditions of high enthalpy sufficient for auto-ignition (> 1,800 K stagnation temperature). This is because static temperature and pressure of the fuel/air mixture in the model scramjet will increase as the flow travels through the internal flow channel confining a train of oblique shockwaves. In addition, the shock-induced flow deceleration and boundary layer developments on the internal surfaces will provide slow flow area in the downstream partially-premixed region helping flame ignition and stabilization. When a downstream flame is ignited, the combustion heat release and downstream pressure build-up will trigger flame propagation toward upstream until the flame finds a location for anchoring where flame displacement speed is identical to approaching flow speed. In general, the approaching flow gets faster as the flame moves upstream because the approaching flow decelerates while traveling through the model scramjet or an internal flow channel. When the flame anchors at a location in the partially-premixed zone, the behavior of the quasi-stable (stable during the rest of the test time after anchoring) flame reveals ***characteristics of a premixed flame***. For example, the flame anchors at the furthest upstream location when the overall equivalence ratio (ϕ) is slightly higher than unity that maximizes fuel burning rate of a premixed-flame (as flame images shown in Fig. 4; M = 4.5, T_0 = 2,500 K and P_0 = 100 kPa in the freestreams). Otherwise, a non-premixed flame ignited on the windward side of the fuel jet, often observed with high fuel jet flow rates (stronger fuel jet induced bow shock), diminishes the influence of fuel concentration on the location of the quasi-stable partially-premixed flame (Fig. 4, ϕ > 2.26). In the presence of the non-premixed flame, the partially-premixed flame stabilizes at a location adjacent to the cavity flameholder regardless of the overall fuel concentration. We conjecture that the non-premixed flame pilots a partially-premixed flame so that the flame is stabilized behind the fuel jet near the cavity flameholder. The jet flame (non-premixed flame) piloting a downstream partially-

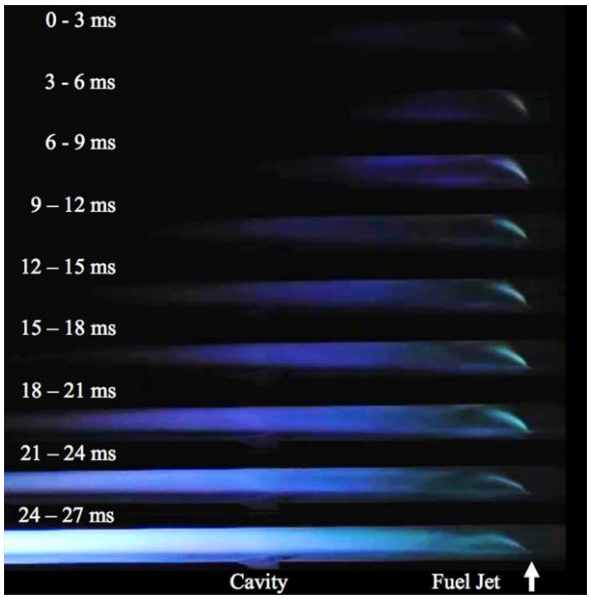

Figure 5. A set of time sequential flame images with a Mach 9 freestream of T_0 = 3,500 K, P_0 = 340 kPa and ϕ = 3.3 (12° upper lip angle).

premixed flame is illustrated more clearly in time sequential flame images of Fig. 5 when freestream Mach number, overall equivalence ratio (ϕ) and flow enthalpy are higher, M = 9, ϕ = 3.3, and T_0 = 3,500 K, respectively. In this case, upper lip angle of the inlet is increased to 12° from 6° to induce stronger incident shockwaves into the isolator. As shown in the 3 – 6 ms panel of Fig. 5, a non-premixed flame appears immediately after the fuel jet injection even before the fuel jet is fully developed, and the flame stretches downstream to pilot a partially-premixed flame (12 – 27 ms panels of Fig. 5). As shown in Fig. 5, under the high-enthalpy and high Mach number conditions where the ignition and stabilization of non-premixed flames are relatively easy, the non-premixed flame dominates flame dynamics in cases piloting downstream partially-premixed flames with sufficiently long combustors such as the one used in this study.

In this study, we focus more on the behavior of the premixed/partially-premixed flames although the non-premixed flame on the fuel jet plays a critical role significantly influencing the flame dynamics as reported above. This is because the premixed flame consumes majority of the injected fuel, therefore, determines the overall combustion efficiency and performance of the engine. The non-premixed flames are observed more often at higher freestream Mach number conditions (Mach 6 and 9) that increase jet-induced bow shock strength prompting ignition of non-premixed jet flames.

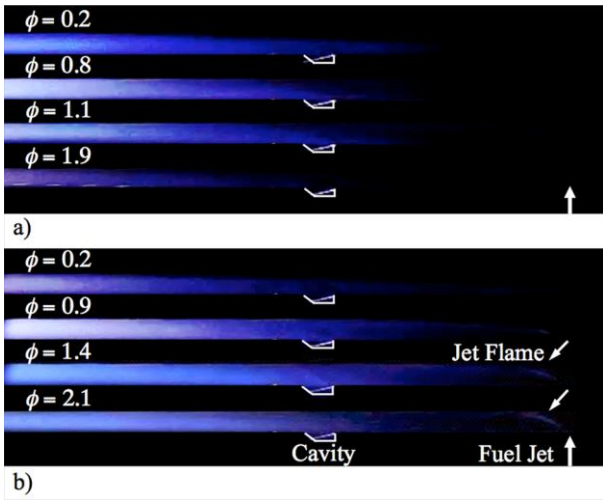

Figure 6. Quasi-stable ethylene flames with Mach 6 freestreams of a) T_0 = 2,300 K, b) T_0 = 2,500 K at P_0 = 340 kPa and ϕ = 0.2 – 2.1 (12° upper lip angle).

Based on the observations under various freestream Mach number conditions (4.5, 6, and 9), as the Mach number increases, the behavior of the quasi-steady and partially-premixed flame generally gets less sensitive to the overall fuel concentration (overall equivalence ratio ϕ). It is

presumed that the partially-premixed flame behaves more like a non-premixed flame with the increased freestream Mach number. The images of partially-premixed flames in Mach 6 flows are presented in Fig. 6 where freestream stagnation temperatures are 2,300 K and 2,500 K in Figs. 6a and 6b, respectively. It is noteworthy that no jet flame appears at T_0 = 2,300K, and the partially-premixed flame is ignited at an extremely lean condition (down to ϕ = 0.2). This would be primarily due to the incomplete fuel/air mixing in the region, and the local fuel concentration near the flame front would probably be sufficiently high (e.g., stoichiometric mixture fraction) for sustaining combustion reactions. This implies that the flame observed in a region downstream of the fuel jet at Mach 6 is a partially-premixed flame that is closer to a non-premixed flame rather than a fully-premixed flame. The degree of fuel/air mixing at the flame front will vary depending on the flow conditions including flow speed and turbulent intensity. As the freestream Mach number or flow speed increases, the flow residence time in the model scramjet or mixing time prior to flame ignition will decrease resulting in less fuel/air mixing at the flame location. Therefore, ***the partially-premixed flame will have more of the characteristics of a non-premixed flame as the freestream speed increases***. Otherwise, once a non-premixed flame on the windward side of the fuel jet appears at the higher flow enthalpy of 2,500 K in Fig. 6b (ϕ) = 0.9 – 2.1 panels), the jet flame pilots the partially-premixed flame that moves upstream toward the fuel jet. This observation is consistent with the flame dynamics seen at Mach 4.5 in Fig. 4.

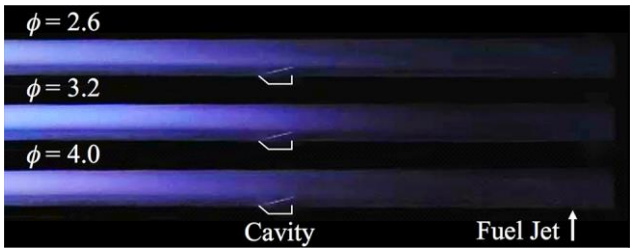

Figure 7. Quasi-stable ethylene flames with a Mach 9 freestream of T_0 = 1,950 K, P_0 = 490 kPa and ϕ = 2.6 – 4.0 (12° upper lip angle).

To investigate the behavior of the partially-premixed flames at M = 9, the flow enthalpy is further reduced (T_0 < 2,000 K) to prevent the non-premixed jet flame ignition at the highest freestream Mach number in this study. Flame images in Mach 9 freestream flows of 1,950 K stagnation temperature are presented in Fig. 7. The overall equivalence ratio (ϕ) is varied between 2.6 to 4.0 where the partially-premixed flame stabilizes in the imaging region without a jet flame. It is obvious that the overall fuel concentration does not remarkably affect the location of the partially-premixed flame even without a jet flame piloting the partially-premixed flame. Presumably, the temperature (static) in the post-shock region (jet-induced bow shock) is not high enough to ignite a non-premixed jet flame under the low flow enthalpy condition while the bow shock is stronger (higher static pressure ratio (compression) across the bow shock) than that in Mach 4.5 and 6 freestream flows.

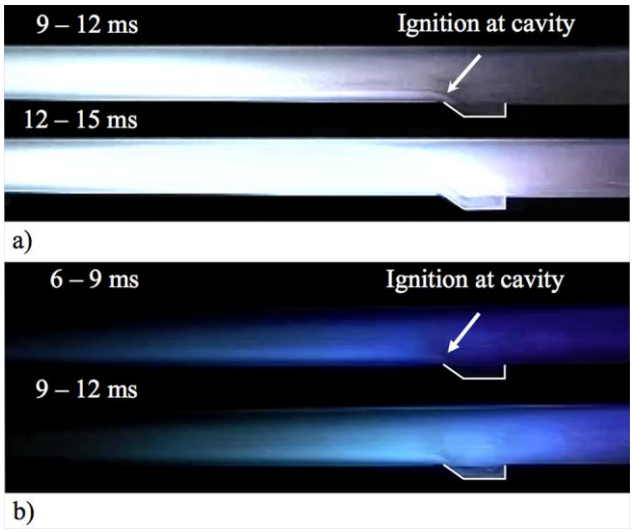

Figure 8. Near cavity ethylene flames with overall equivalence ratio a) $\phi = 1.34$ and b) $\phi = 3.51$ (Mach 4.5 freestream of T_0 = 2,500 K and P_0 = 100 kPa, 6° upper lip angle).

Geometric alterations on the combustor surface such as a wall cavity flameholder can also affect the ignition and stabilization of a partially-premixed flame. The flame-holding capability of the cavity varies with freestream Mach number, overall equivalence ratio (particularly at Mach 4.5), and flow enthalpy. With the Mach 4.5 freestream of 2,500 K stagnation temperature, the partially-premixed flame stabilizes near the cavity in a wide range of overall equivalence ratio ϕ = 0.93 – 3.51 as shown in Fig. 4. The wall cavity provides a slow flow region with relatively high static temperature/pressure that helps flame ignition and stabilization serving as a radical pool supplying radical species to the region adjacent to the flameholder. Furthermore, the cavity can enhance fuel/air mixing by elongating flow residence time and recirculating the mixture in the cavity. Presumably, the flame stabilization near the cavity observed in Fig. 4 is benefited by the radical production/supply from the cavity as well as the prolonged mixing time. The wall cavity can ignite flames when the fuel entrainment into the cavity region is sufficient. The cavity flame ignition at M = 4.5 is observed under relatively fuel-rich conditions as shown in Fig. 8a ϕ = 1.34 and 8b ϕ = 3.51. Interestingly, partially-premixed flames are ignited at both locations downstream and in the cavity at ϕ = 1.34 (Fig. 8a), then the downstream partially-premixed flame propagates upstream and merges with the cavity-ignited flame (12 – 15 ms panel in Fig. 8a). Otherwise when overall ϕ = 3.51, a partially-premixed flame first appears on the cavity ramp (6 – 9 ms panel in Fig. 8b) and stretches downstream to hold a flame anchoring near the cavity (9 – 12 ms panel in Fig. 8b). The cavity-induced shock on the cavity ramp and the elevated static pressure/temperature in the cavity would directly and indirectly trigger the cavity ignition in the cases presented in Fig. 8.

Based on the flame behaviors observed under the various flow conditions in Figs. 4 through 8, one can conclude that the cavity flame-holding will be particularly necessary when i) the flow enthalpy is low (e.g., T_0 < 2,000 K and M < 6 with the current model scramjet configuration), and ii) a non-premixed flame piloting a partially-premixed flame is not ignited on fuel jets. In practice, the cavity flame-holding would be essential in stabilizing a partially-premixed flame while a scramjet accelerates prior to reaching hypersonic flights above Mach 5. Once the flight Mach number exceeds 6, the role of the cavity

flameholder would be less critical due to the high Mach number and high-enthalpy flows capable of igniting and stabilizing the partially-premixed and non-premixed pilot flames.

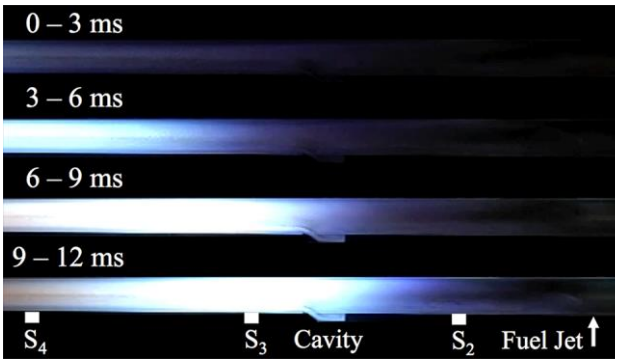

Figure 9. Time sequential flame images with a Mach 4.5 freestream of T_0 = 2,650 K and P_0 = 100 kPa at ϕ = 0.93 (reference time 0.150 s, 6° upper lip angle).

Flame Propagation: Transient ethylene flame propagation through the model scramjet is characterized using a fast camera and five couples of pressure/temperature (P/T) sensors (S1 – S5 in Fig. 3a) mounted flush with the internal surface of the model scramjet. Once a partially-premixed flame is ignited at a location downstream of the fuel jet, the flame starts to propagate upstream until it reaches a location appropriate for stable combustion reactions. The flame propagation speed with Mach 4.5 freestream flows is estimated for investigating the influence of fuel concentration and freestream flow conditions (e.g., temperature and oxygen concentration) on the unsteady behavior of the partially-premixed ethylene flame. The partially-premixed ethylene flame interacts with the compressible flow environment to alter the flow field in scramjets. For example, the ignition of the partially-premixed flame induces flow separation on the combustor surface due to the combustion heat-release and the downstream pressure build-up. In the separated flow region, the flow is in subsonic regime and the flow above the region will be decelerated to increase static pressure. Then the separated flow will reattach on the surface afterwards to re-accelerate the internal scramjet flow, therefore the static pressure will decrease again. The location of the highest pressure (local maximum) where the flow is separated from the combustor surface is called thermal throat. Presumably, the strongest combustion reactions of the partially-premixed flame will occur in a region adjacent to the thermal throat. In this study, the locations of a thermal throat and partially-premixed flames are traceable with the sensors providing the static pressure (P) and surface temperature (T) traces on the internal surface of the model scramjet. Local maxima of surface pressure distributions will depict the thermal throat, and the P and T will rise simultaneously when a partially-premixed flame arrives at a sensor location.

Typical flame structures and pressure/temperature traces in the model scramjet are presented in Figs. 9 and 10. In these figures, freestream Mach number, stagnation temperature and overall equivalence ratio in the supersonic combustor are 4.5, 2,650 K and 0.93, respectively. As soon as the ethylene fuel is injected into the combustor at 0.150 s, a partially-premixed flame appears and propagates toward upstream to be stabilized at a location between S2 and S3 (as the time sequential flame images shown in

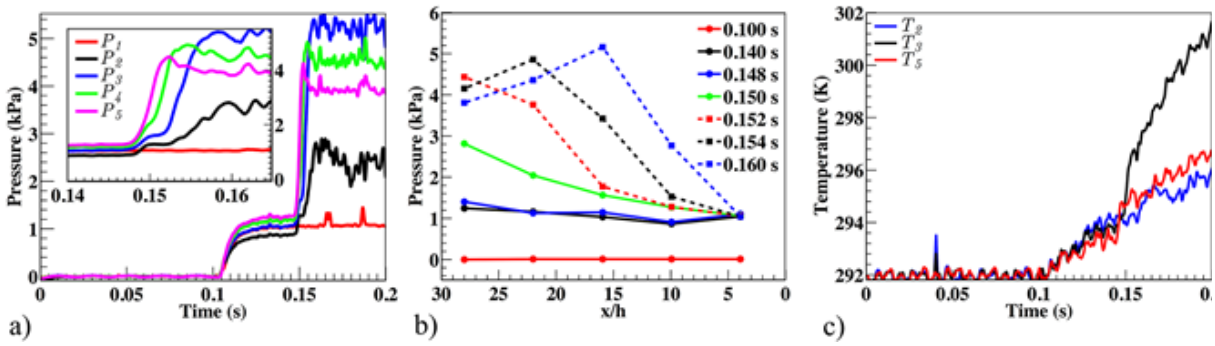

Figure 10. a) Surface pressure traces, b) spatial pressure distributions and c) surface temperature traces with a Mach 4.5 freestream of T_0 = 2,650 K and P_0 = 100 kPa at ϕ = 0.93 (x = 0 at the inlet lip).

Fig. 9). This observation is consistent with the pressure traces shown in Figs. 10a and 10b. Sudden pressure rises are observed in a sequence from S5 through S1, presumably indicating flame ignition near S5 and transient flame propagation toward upstream. When the flame is stabilized (approximately at 0.160 s), the pressure distribution in the model scramjet reaches a steady-state with the maximum static pressure P at S3 (P1 < P2 < P3 > P4 > P5, as shown in Figs. 10a and 10b). This is a typical pressure distribution with a thermal throat near S3. During the flame residence at the location, T3 (surface temperature at S3) increases rapidly (Fig. 10c) due to the significant combustion heat release and increased static pressure at the location. As shown in Fig. 9, the stabilized partially-premixed flame is near S3 where the surface pressure is the highest (Fig. 10b). This implies that the thermal throat is near the primary combustion zone, presumably involves the flow separation due to the intensive combustion reactions and downstream pressure build-up. Otherwise, no significant flame chemiluminescence is observed at S2 (Fig. 9) while the relatively mild pressure rise shown in Fig. 10a indicates flow separation at the location upstream of the thermal throat. This is because the separated flow region at the thermal throat in subsonic regime extends upstream. In addition, it is obvious that the flow upstream of the fuel jet (the pressure trace at S1 (P1) as shown in Fig. 10a) is not disturbed by the jet injection or the downstream flame ignition/propagation/heat release.

Table 1. Propagation speeds of partially-premixed flame with freestream of M = 4.5

Case	O_2%	T_0,	V_∞,	ϕ	V_{flame}, m/s
1	21	2545	1954	2.49	15
2	21	2737	2029	1.34	74
3	21	2780	2038	1.67	55
4	21	2816	2025	2.26	59
5	21	2875	2050	2.66	50
6	21	2875	2050	1.39	83
7	38	1778	1638	0.63	118
8	43	1792	1651	0.60	163

Flame propagation speed measurement results (from S4 to S3) are provided in Table 1. As shown in the table, increased total temperature and oxygen concentration accelerate the flame propagation speed. For example, due to the increase of total temperature by 330 K (see cases 1

and 5 of 2,545 K and 2,875 K stagnation temperature, respectively), the propagation speed is significantly increased from 15 m/s to 50 m/s. The influence of oxygen concentration that represents the effect of reaction speed or burning rate can be seen in cases 7 and 8 with the increased oxygen contents, 38% and 43%, respectively. The flame propagation speed is significantly increased by the oxygen concentration change from 38% to 43 % with the same fuel injection rate and freestream total temperature.

Predicting flame propagation behavior with both the temperature and oxygen concentration changes requires consideration of various relevant parameters such as fuel burning rate, air/fuel mass flow rates, and freestream flow momentum that are associated with combustion chemistry and fluid dynamics in the internal flow channel. The flame propagation speed is significantly increased by oxygen enrichment (21% to 43%) with reduced total temperature (2,900K to 1,800K) as shown in cases 6 and 8. The propagation speed in case 8 (163 m/s) is about twice as fast in comparison with that of case 6 (83 m/s). This increased propagation speed is not simply due to enhanced combustion chemistry that are accelerated by the oxygen enrichment, but also involves the increased fuel and freestream mass flow rates. If the combustor completely consumes the injected fuels in both cases, combustion heat release rate of case 8 would be significantly higher than that in case 6. In the process, downstream pressure build-up enhanced by the faster combustion heat release would accelerate the flame propagation toward upstream in case 8 even with the increased freestream momentum hindering the flame propagation.

In addition, it was found that the flame propagation is the fastest when overall equivalence ratio (ϕ) is approximately 1.3 (as shown in cases 2 and 6) under a fixed freestream flow condition. Obviously, the propagation speed decreases as the fuel injection becomes excessive (compare cases 2 and 3 or cases 5 and 6), which is a typical characteristic of premixed flames. Nevertheless, it seems like that the flame propagation speed is less sensitive to fuel concentration under fuel-rich conditions ($\phi > 1.5$) as shown in cases 3 and 4. Overall equivalence ratio was increased from 1.67 (case 3) to 2.26 (case 4) in a nominally identical flow, however, the flame propagation speed is decreased only by 7%, from 59 m/s to 55 m/s. This is consistent with the flame behavior observed in Fig. 4 that becomes less sensitive to fuel concentration when a non-premixed flame appears on the fuel jet at $\phi > 1.5$.

Inlet Unstart: The inlet unstart phenomenon is optically observed simultaneously with pressure/temperature measurements on an internal surface of the model scramjet. In this study, rapid pressure rises at the inlet and reverse flows fuelling flames in a region upstream of the fuel jet indicate the inlet unstart. Excessive heat release from combustion reactions causes thermal choking to trigger inlet unstart. The combustion heat release is primarily from a partially-premixed flame that behaves largely depending on overall fuel concentration particularly in Mach 4.5 freestream flows as shown in this study. The partially-premixed flame induces the formation of a thermal throat that eventually chokes the flow to trigger inlet unstart. Nevertheless, overall fuel concentration in scramjets is not the only critical parameter

in the inlet unstart mechanism. In practice, fuel concentration will be determined by fuel injection rate and air flow rate through the engine that depends on flight velocity/altitude and atmospheric pressure/temperature. Even if all freestream flow parameters upstream of the combustor except for the fuel injection rate are constant, the fuel injection rate can alter several critical engine operation parameters that significantly affect flame propagation and the inlet unstart phenomena. As the overall equivalence ratio (ϕ) increases from zero to unity with an increasing fuel injection rate, the chance for inlet unstart to occur will increase because i) total combustion heat release, ii) local fuel burning rate, and iii) mass loading via fuel injection will increase simultaneously. Nevertheless, according to our previous studies with the current model scramjet configuration, inlet unstart is unlikely to occur under the fuel-lean ($\phi < 1$) conditions.

As the overall ϕ (or fuel injection rate) further increases ($\phi > 1$), the total combustion heat release will not increase, but the mass loading via fuel injection will monotonically increase, and the local burning rate at flame fronts will increase and decrease. It is well known that excessive mass loading can choke the flow even without any combustion heat release. In addition, enhanced burning rate at a stabilized location will elevate local temperature to potentially prompt thermal choking.

The scramjet operations of cases 2 through 6 in Table 1 do not induce inlet unstart, while the flow undergoes inlet unstart in case 1 with relatively lower enthalpy and higher fuel concentration. This is because the total combustion heat release in case 1 is the highest (both of the fuel and air mass flow rate are the highest) out of the 6 cases (1 – 6). The unstart in this case is primarily from combustion heat release, not fuel mass loading because the model scramjet re-starts with further increment in fuel injection rate that adds mass loading but reduces combustion heat release (slower burning rate). In the test facility used in this study, the reduction of flow enthalpy at a fixed Mach number (fixed C/D nozzle geometry) and total pressure will result in increasing total mass flow rate, therefore

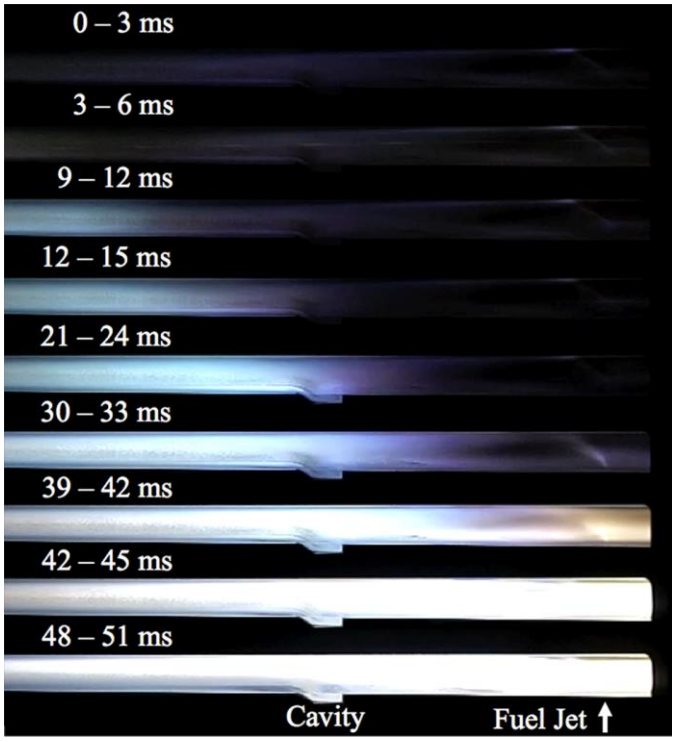

Figure 11. Time sequential flame images with a Mach 4.5 freestream of T_0 = 2,545 K and P_0 = 100 kPa at ϕ = 2.49 (reference time 0.145 s, 6° upper lip angle).

total combustion heat release will increase under the fuel-rich conditions (ϕ > 1) with the reduced freestream temperature assuming complete oxygen consumption in the mixture. Total combustion heat release in cases 7 and 8 are even higher than that of case 1 due to the reduction of total temperature and oxygen enrichment in flows, therefore, the inlet unstart occurs in both the cases 7 and 8.

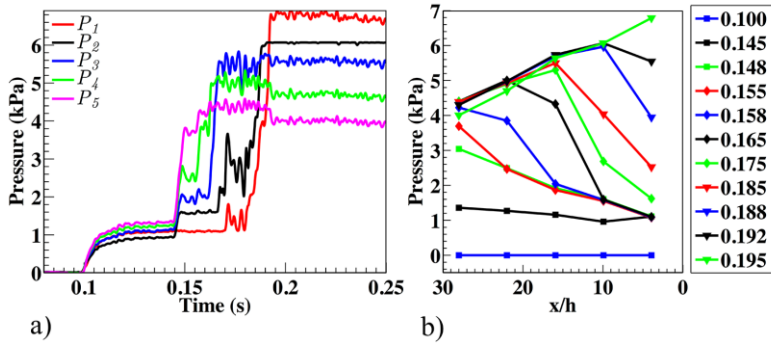

Figure 12. a) Surface pressure traces and b) spatial pressure distributions with a Mach 4.5 freestream of T_0 = 2,545 K and P_0 = 100 kPa at ϕ = 2.49 (x = 0 at the inlet lip).

Figure 11 shows a set of time sequential flame images of case 1 with a reference time 0.145 s when the fuel jet is injected. The flame ignited far downstream (3 – 6 ms panel) propagates upstream (9 – 24 ms) to reach the fuel jet. In panels at 30 – 51 ms, a flame upstream of the fuel jet is observed depicting that the flow in the inlet region is in subsonic regime. Obviously, a reverse flow fuelling the upstream flame exists which is one of the inlet unstart indicators used in this study. The orange color flame emission (39 – 42 ms panel) upstream of the fuel jet would be due to soot formation from high temperature and fuel-rich combustion reactions occurring in the inlet region. The rapid flow deceleration at the inlet will elevate the static temperature in the region up to the stagnation temperature prior to the fuel burning, and the incoming air flow spillage at the inlet caused by the flow choking will significantly reduce the oxygen supply into the inlet area to make the flame even richer. After the flame reaches the inlet region (42 – 51 ms), the flame emission is so strong to saturate the camera CCD. This unsteady unstart flame dynamics is also resolved by the pressure traces shown in Fig. 12. The sudden pressure rises depicting the flame arrival at the sensor locations are observed in a sequence from downstream (S5) to upstream (S1) in Fig. 12a. Figure 12b illustrates the spatial pressure distribution along the model scramjet that changes over time. The location of the highest wall pressure indicating thermal throat moves from downstream to upstream to reach S1 placed at the furthest upstream in the inlet. This implies that the thermal throat is advancing further upstream toward inlet lip to choke the scramjet flow, prompt disgorgement of an unsteady shock system, and induce formation of a normal shockwave in front of the inlet. Otherwise, the thermal throat stays somewhere in the scramjet combustor without choking the flow under normal scramjet operation conditions as shown in Figs. 9 and 10.

1-3) Simultaneous Fuel Concentration and Gas Density Measurements in a Supersonic Combustor

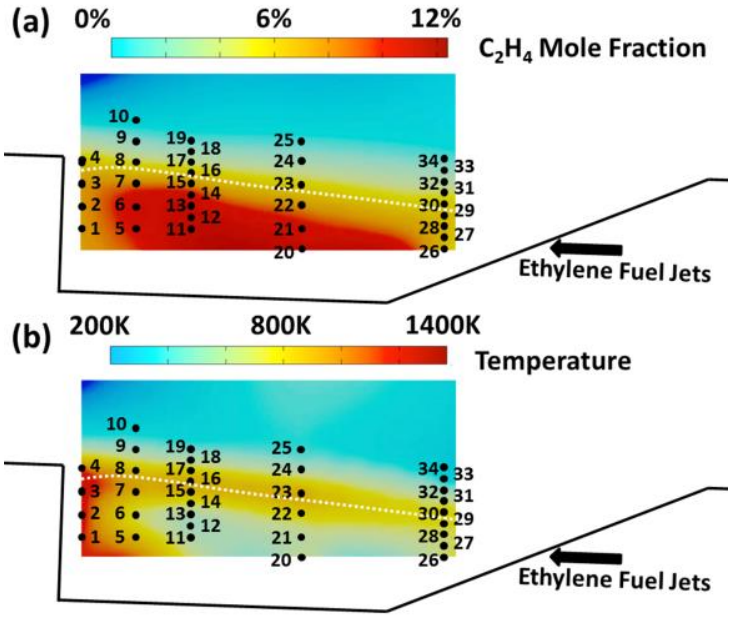

Figure 13. 2-D (a) concentration and (b) temperature fields measured in and above a cavity flameholder in the RC-19 supersonic wind tunnel with Mach 2 freestream flows.

Measuring flow properties such as species concentration, pressure, temperature, and gas density in high-speed compressible flows is challenging because insertion of a physical probe can cause significant flow disturbances (e.g., shockwaves) that can alter the flow properties. Therefore, optical methods have been developed and used in high-speed flows, as they provide qualitative and quantitative measures without perturbation. Spontaneous Raman scattering and Rayleigh scattering provide species (e.g., component concentration) and gas density. However, these methods require laser systems delivering high pulse energy (>400 mJ/pulse), and the complexity of the measurement systems may limit their application to laboratory environments, as opposed to test environments. Alternatively, Laser-Induced Breakdown Spectroscopy (LIBS) produces high emission intensity and minimal system complexity and requires only moderate laser energy (≥ 100 mJ/pulse). LIBS is a point measurement method using a focused laser beam to generate plasma of minimal volume (< 1 mm^3) serving as a virtual measurement probe. Atomic emission line intensities of the plasma probe are sensitive to species concentration and are therefore used as concentration indicators in LIBS.

n-LIBS and d-LIB for Concentration and Density Measurements: Through the collaboration with AFRL (Dr. Campbell D. Carter), a nanosecond-gated LIBS (n-LIBS) method was developed to measure species concentration in a reactive flow. This newly developed n-LIBS technique minimizes measurement time required for extracting fast-decaying atomic emission lines. The minimized measurement time (< 100 ns) enables application of the n-LIBS in turbulent supersonic flows that quickly move and smear plasma probes to increase measurement uncertainty. In addition, the pressure dependence of the n-LIBS was investigated; understanding this pressure dependence is essential for measurements in compressible flow environments. Furthermore, a new method of gas density measurement utilizing the laser-induced

breakdown (d-LIB) was proposed and used in the high-speed environment. It was shown that the laser pulse energy scattered/absorbed by the plasma probe, defined here as plasma energy (PE), is sensitive to gas density. A single laser shot allows both the n-LIBS and d-LIB diagnostics, enabling simultaneous fuel concentration and gas density measurements that were used for measuring flow properties in a cavity flameholder in a supersonic (Mach-2 freestream) wind tunnel at Wright Patterson Air Force Base (RC-19), see Fig. 13.

Direct Spectrum Matching (DSM) Method: A direct spectrum matching (DSM) method for improving the accuracy of the n-LIBS technique in turbulent reacting environments was newly proposed. In this new method, the laser-induced breakdown spectrum recorded in the target flow was directly matched with a spectrum out of a database consisting of various emission spectra recorded under well-defined conditions in a range of gas density and composition. It was shown that the wavelength, intensity and line width of the atom/ion emission lines in the spectrum indicate atom composition and gas density that are independent of parent molecular species in the target flow. Once a matching spectrum (within 550 nm – 830 nm containing O, H, N, and C lines) in the database of a known gas condition is found, the concentration and gas density at the location of the breakdown can be accurately derived. This new method was successfully tested at Wright Patterson Air Force Base (Dr. Campbell D. Carter and Dr. Timothy Ombrello) revealing 3D flow property fields in a supersonic combustor of the Research Cell 19 (RC-19). As for the prior n-LIBS tests, a 532-nm Nd:YAG laser with 10-Hz pulse repetition rate was used to induce breakdown in fuel/air mixtures for the universal applications.

1-4) Influences of the Freestream Turbulence on the Flame Dynamics

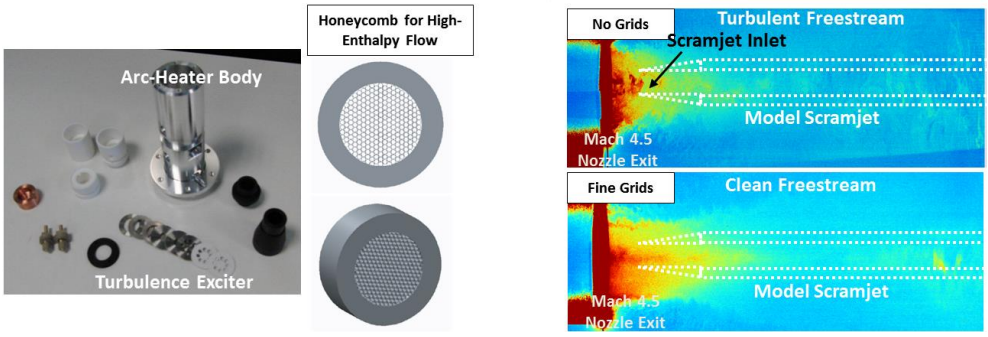

(a) (b)

Figure 13. a) Turbulent exciters and honeycomb designed for turbulent mixing and turbulence control that are located upstream of the C/D nozzle, and b) qualitative freestream turbulence visualization using CO_2 fogs at low enthalpy operation conditions with/without a fine grid.

Freestream turbulence affects combustion chemistry, therefore, burning rate, combustion efficiency, and shock-flame/boundary-flame interactions. Consequently, combustion stability and flammability limit in the high-Reynolds environments will be significantly influenced by the freestream turbulence, thus quantifying/controlling the turbulence in the ground test facility (ACT-1) is extremely critical. We have conducted freestream turbulence control experiments using turbulent screens and a rapid flow contraction. Multiple turbulent exciters, honeycombs and meshes (Fig. 13 a)) that are implemented upstream of the converging/diverging (C/D) nozzle of the tunnel were used to control freestream turbulence and provide uniform turbulence in the entire flow area upstream of the model scramjet. It was confirmed that this traditional turbulence control method is very effective especially with sufficiently large C/D nozzle throats that are not fully suppressing (laminarizing) turbulence originating from the upstream turbulence exciters. The freestream turbulence level in the open test section of the facility was qualitatively evaluated

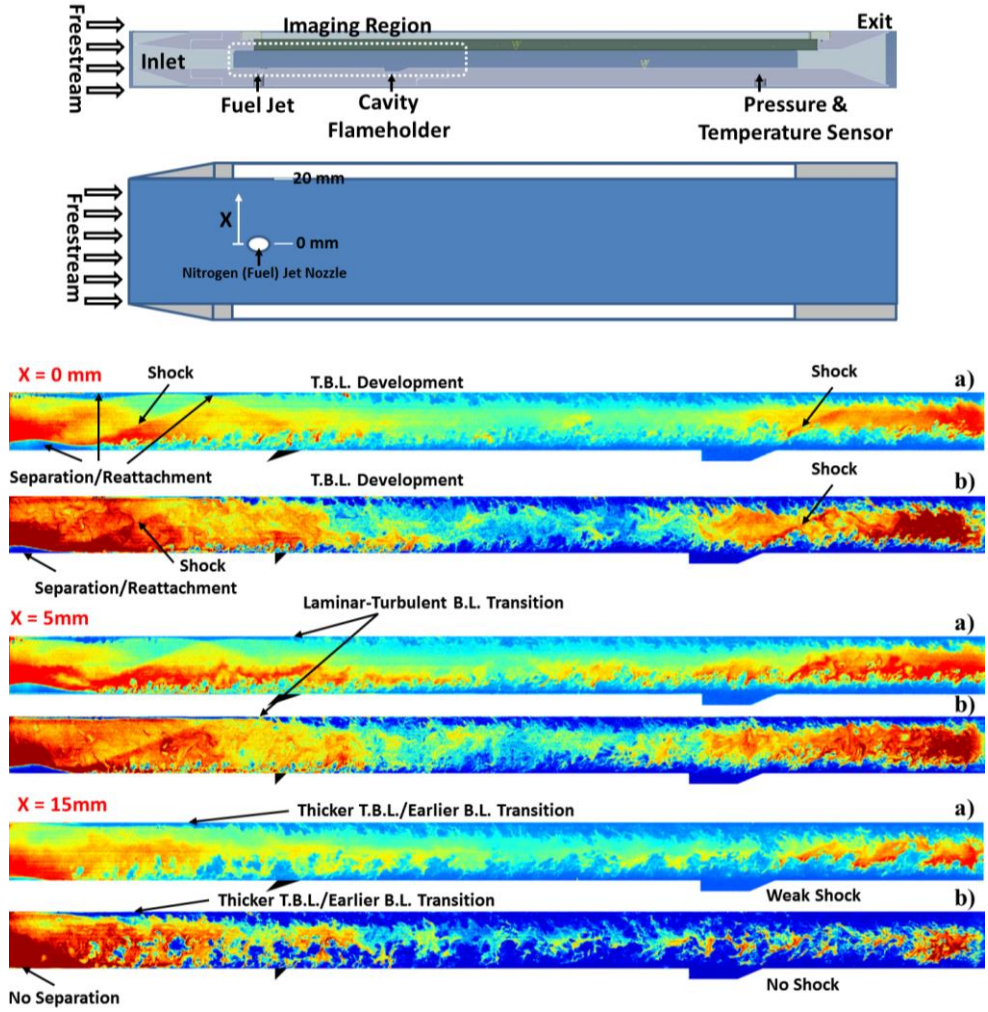

Figure 14. Scramjet flows without a fuel jet visualized by condensed CO_2 particles a) with and b) without fine mesh grids upstream of the C/D nozzle of ACT-1. Freestream Mach # = 4.5.

(Fig. 13 (b)) using condensed CO_2 particles seeded into low enthalpy freestream flows. The flow field in the model scramjet was visualized by capturing scattered laser beam (2D sheet) from condensed CO_2 particles at Ma = 4.5 freestream conditions, and the laser sheet parallel to the freestream is moved from the center of the scramjet toward the side wall to scan the 3D flow structures. Interesting sidewall boundary layer structures, shock-boundary layer interactions, shock structures, laminar-turbulent boundary layer transition were successfully visualized instantaneously (10 ns laser illumination), and the influences of the freestream turbulence on the representative flow features/interactions were qualitatively evaluated (Fig. 14). The visualization with fuel jets (Fig. 15) also indicated that the new expanding supersonic fuel jet implemented on the model scramjet enhances fuel/air mixing to provide premixed/partially-premixed environment in the region downstream of the jets.

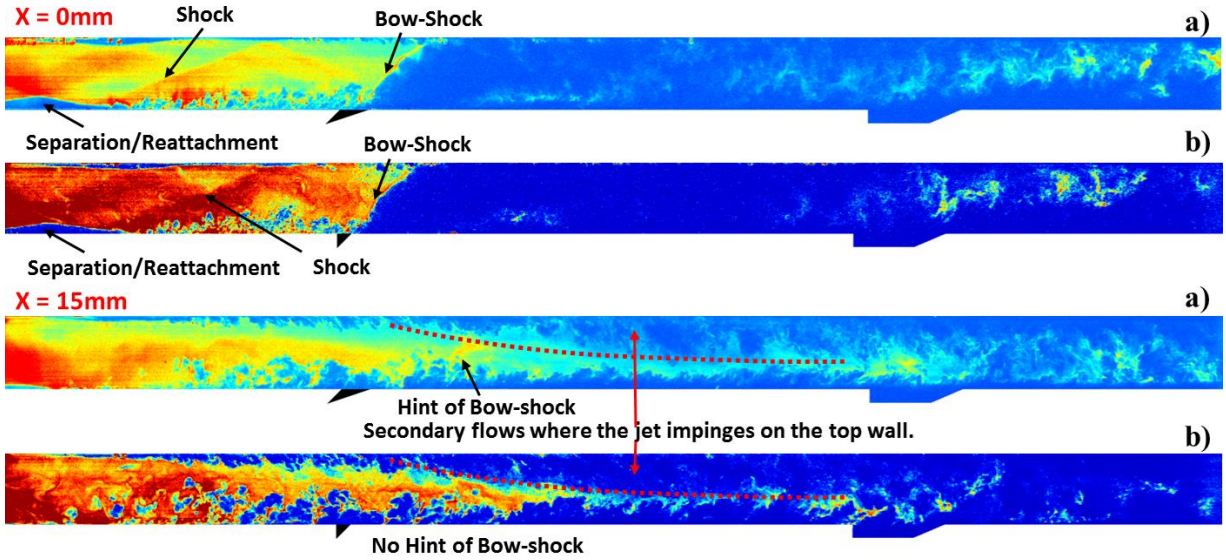

Figure 15. Scramjet flows visualized by condensed CO_2 particles with nitrogen jet injection a) with and b) without fine mesh grids upstream of the C/D nozzle of ACT-1. Freestream Mach # = 4.5.

<u>Freestream Turbulence Control for High-Enthalpy Flows:</u> It is obvious that the freestream turbulence significantly affects the flow structures in the supersonic combustor, thus presumably the combustion dynamics (non- and partially-premixed) will be altered accordingly. Nevertheless, controlling turbulence with the meshes is impossible when with the high-enthalpy flows exceeding 2,000K that are required for the scramjet combustion tests. Therefore a rapid flow contraction that has been widely used to effectively reduce freestream turbulence was chosen for controlling the high-enthalpy combustion test facility (Fig. 16 (b)). The flow contraction component was inserted between the turbulent exciter and the C/D nozzle throat (Fig. 16 (a)).

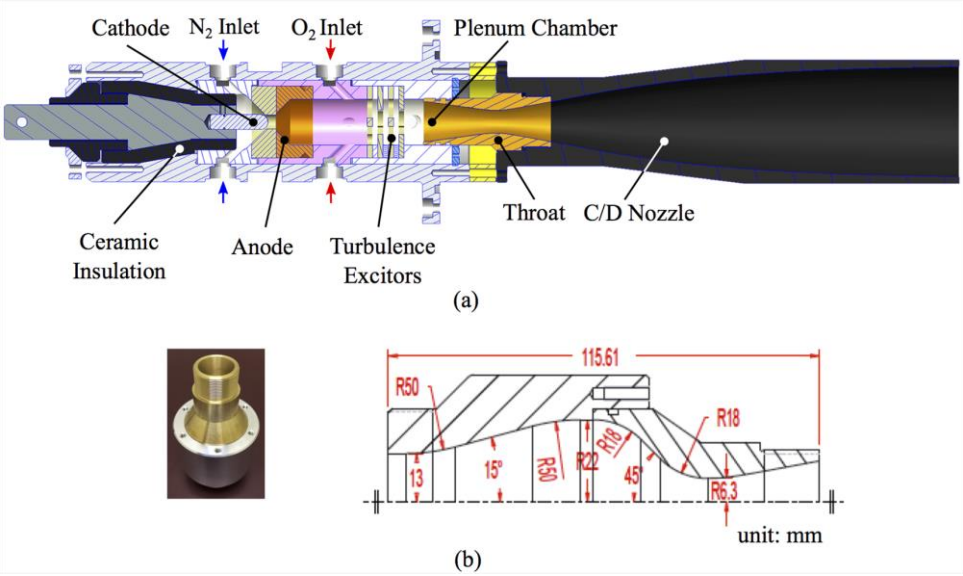

Figure 16. The structure of (a) the arc-heating unit connected to the C/D nozzle and (b) the rapid flow contraction component.

Here, two representative freestream turbulence cases are provided and compared. In order to indirectly evaluate the freestream turbulence level, freestream pressure fluctuations were recorded on a plane 1 cm downstream from the C/D nozzle exit in the high and low turbulence modes using a pressure probe; the freestream turbulence would be amplified by a normal shockwave appearing in front of the probe head. The high turbulence mode was produced using a 4:1 contraction ratio inlet for the Mach 4.5 nozzle, whereas for the low turbulence mode, the contraction ratio is increased to 12:1 via a rapid flow contraction component. Total pressure and temperature of the flows are kept constant in both cases, while

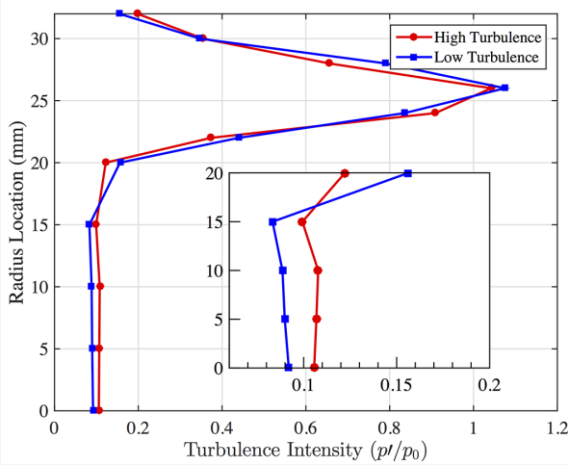

Figure 17. Distributions of pressure fluctuations on a plane 1 cm downstream from the C/D nozzle exit.

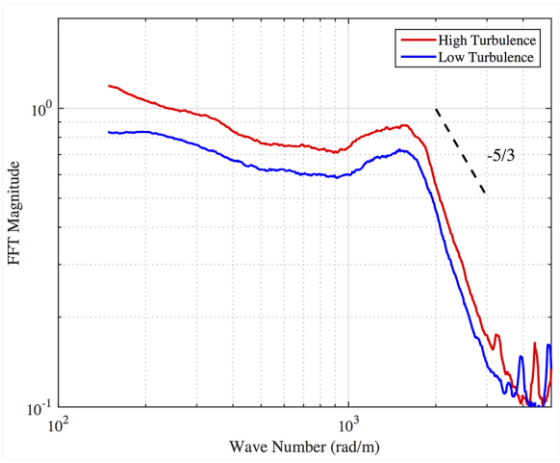

Figure 18. FFT plots of the pressure fluctuations measured 1 cm downstream from the C/D nozzle exit.

the post-shock pressure traces are recorded at multiple locations along the radial direction from the center of the core flow. A nominal intensity of the freestream pressure fluctuation is defined as the ratio of the root mean square of the pressure fluctuation component (p') to the mean pressure (p_0) behind the normal shock. As shown in Fig. 17, the nominal pressure fluctuation in the core flow area is around 12% in high turbulence mode and 8% in low turbulence mode. The core flow area is bounded by the shear layer originating from the rim of the C/D nozzle exit that causes sudden increase of the pressure fluctuation at approximately 20 mm from the center. It is consistent with previous reports showing that the fast flow contraction with large contraction ratio significantly damped the pressure fluctuations by over 30% of the maximum intensity in freestreams. In the previous studies, the absolute magnitude of the longitudinal fluctuation component decreased as the flow accelerated through the contraction component in incompressible subsonic regime although the lateral component increased. In addition, the pressure fluctuation spectra in wavenumber (frequency) domain with and without the flow contraction are measured and presented in Fig. 18. The remarkable reduction in the pressure fluctuation amplitude with the rapid flow contraction at all wave numbers implies that the freestream turbulence (or velocity fluctuations) at all frequency would be reduced significantly as well. It is consistent with previous observations that the spectrum of the isotropic turbulence produced by the screens can be altered in amplitude and frequency by a rapid distortion of the flow. It is noteworthy however that these measurements are conducted at a room temperature condition, therefore the turbulence dissipation toward the high frequency regime will be faster in arc-heated high-enthalpy flows since the viscosity will be increased in the high temperature flows.

Turbulence Influences on the Turbulent Flame Dynamics: Freestream turbulence can enable stable combustion in a harsh high-speed environment such as that in a scramjet combustor, particularly more effective for premixed or partially-premixed flames. This is because the turbulence enhances both the fuel/air mixing and turbulent flame speed far above the laminar flame speed. The premixed or partially-premixed flame in a high-speed freestream stabilizes or anchors at a location when the flame displacement (or propagation) speed is balanced with the speed of approaching flow at the location. In general, turbulence and local fuel concentration determine the flame displacement speed, and the turbulence affects the local fuel concentration and its gradient where fuel/air mixing is incomplete, i.e., partially-premixed condition. On the other hand, the flame location can be simply dictated by the combustor geometry and/or fuel jet location. As shown in the previous section, 1-2) Turbulent Ethylene Flame Dynamics in a Model Scramjet, three major flame-anchoring locations were identified with the same experimental setup that are the locations of 1) the fuel jet and 2) the cavity flameholder in addition to 3) the variable anchoring location of a partially-premixed flame. Since the appearance of the fuel jet

stabilized flame on the windward side precedes the fuel/air mixing behind, this jet flame is obviously a non-premixed flame rooted on the jet nozzle. The non-premixed flame ignites when the jet-induced bow-shock is strong enough under a certain freestream enthalpy condition to initiate combustion reactions, therefore the bow-shock strength and the freestream enthalpy rather than the freestream turbulence dominate the jet flame dynamics. Likewise, the cavity-stabilized flame always starts from the cavity and its dynamics is not strongly dependent on the freestream turbulence in comparison with that of the partially-premixed flame. Among the three different flame formations seen in the model scramjet, we first focus on the dynamics of the partially-premixed flame that heavily relies on freestream turbulence. It is because the partially-premixed flame consumes the largest portion of the injected fuel and therefore determines the overall engine performance and combustion stability under various flight conditions. This study initially aimed at revealing the critical role of the freestream turbulence on the flame dynamics primarily of the partially-premixed flames but also of the non-premixed flames often piloting the partially-premixed flames in a supersonic combustor.

The two different freestream turbulence conditions presented above were used to investigate the influence of freestream turbulence on flame dynamics. Throughout the study, freestream Mach number, total pressure and total temperature of the flows were fixed at Mach 4.5, 0.65 bar, and 2,600 K, respectively. Overall flame dynamics and detailed flame structures were resolved by capturing flame chemiluminescence and utilizing OH PLIF. The flame chemiluminescence images and OH-PLIF images taken in freestreams of low turbulence intensity are shown in Figs. 19 (a) and (b), and the images in freestreams of high turbulence intensity are presented in Figs. 20 (a) and (b).

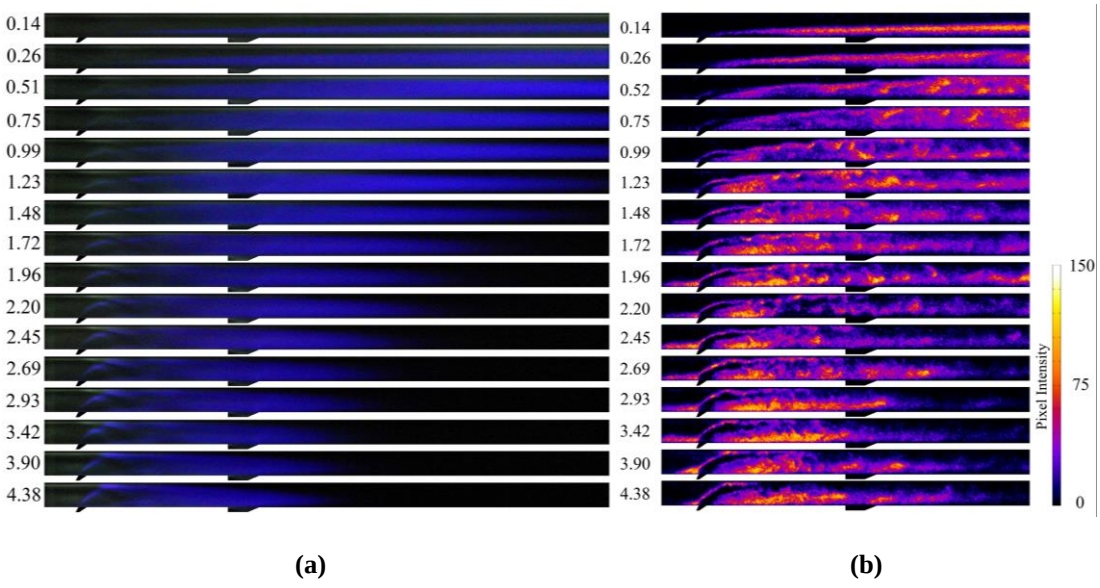

Figure 19. (a) Flame chemiluminescence images and (b) OH PLIF images in Mach 4.5 freestream (low turbulence) at P_0 = 0.65 bar, T_0 = 2,600 K, overall equivalence ratio (ϕ) = 0.14–4.38.

As shown in Fig. 19 (a) in freestreams of low turbulence intensity, a non-premixed jet flame always starts from the fuel jet injection location to be long stretched toward downstream, however no strong partially-premixed flame appears downstream at any fuel concentration condition from 0.1 to 4.4 in overall equivalence ratio. The long-stretched turbulent flame structures on a two-dimensional (2D) plane intersecting the centerline of the model scramjet are visualized instantaneously by OH PLIF as shown in Fig. 19 (b). The non-premixed jet flame on the windward side of the fuel jet is stretched along the interface of the fuel jet and the freestream, and the fuel jet trajectory is wrapped by the flame on the leeward side where the fuel/air mixing occurs within the fuel jet induced wakes. In practice, piloting a stronger partially-premixed flame behind the fuel jet is an ideal role of this non-premixed flame for achieving stable combustion and high combustion efficiency in the high-speed environment. However, the jet flame in this case with the low turbulence intensity does not induce a noticeable downstream flame. The combustion efficiency in this case should be fairly low, which is obviously shown in Figs. 20 (a) and (b) that are images taken under the identical stagnation conditions and overall equivalence ratios but with high turbulence intensity.

In the case of Fig. 20, the freestream turbulence was in the high turbulence mode while all the other physical flow parameters were kept the same as those in the case of Fig. 19 that is in the low turbulence mode. All the images were taken after the flame reaches a steady state. Interestingly, a strong downstream flame appears in a range of overall equivalence ratio (ϕ) = 0.49 – 2.43 as shown in Fig. 20 (a). It is evident that the flame dynamics including the flame anchoring location strongly depends on the

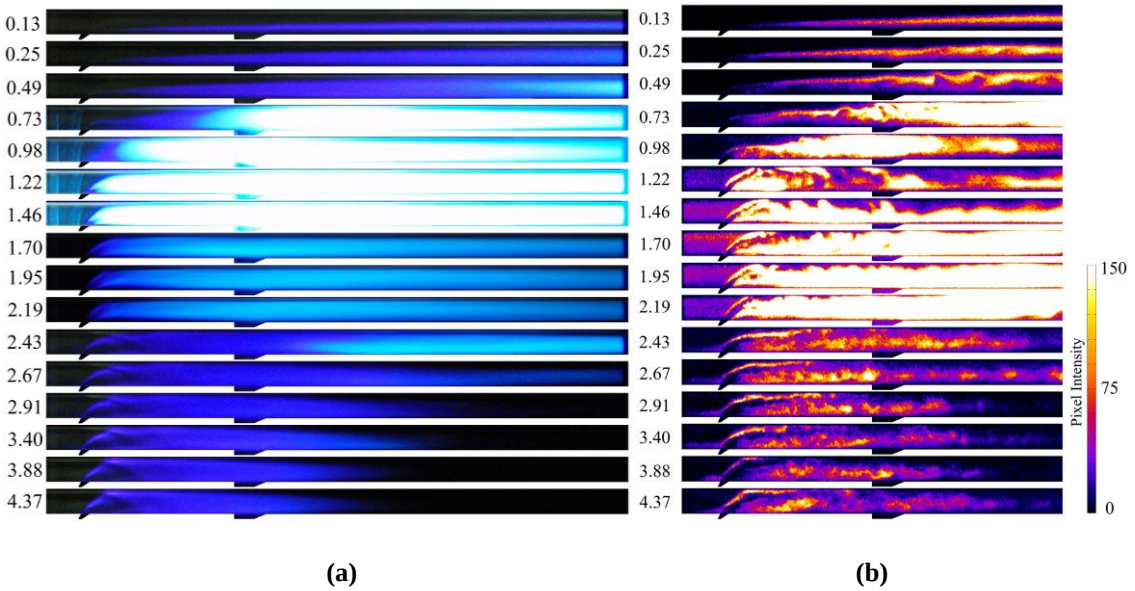

Figure 20. (a) Flame chemiluminescence images and (b) OH PLIF images in Mach 4.5 freestream (high turbulence) at P_0 = 0.65 bar, T_0 = 2,600 K, overall equivalence ratio (ϕ) = 0.13–4.37.

overall equivalence ratio, i.e., the flame advances the furthest upstream when ϕ is slightly above the unity (ϕ = 1.22 and 1.46 in this case). This confirms that the intense flame observed in the images is a partially-premixed flame where the fuel concentration is one of the dominant parameters determining the flame dynamics. In general, the influence of overall fuel concentration on a non-premixed flame is relatively insignificant. It has been observed that the partially-premixed flame usually starts from a further downstream region where the fuel and air are relatively well-mixed and the flow is further decelerated and compressed, and then propagates upstream until anchoring at a stabilization location. Consequently, the intense partially-premixed flame, not seen in the low turbulence intensity case (Fig. 19), can be successfully stabilized by the enhanced freestream turbulence that accelerates both the fuel/air mixing and the turbulent flame speed.

Although the turbulence effect on the non-premixed flame is insignificant in comparison with that on partially-premixed flames, the freestream turbulence does affect the non-premixed flame as well. Non-premixed flame commonly resides on the interface of fuel and air where diffusion dominates molecular level mixing prior to burning. High-frequency and small-scale turbulence can also effectively enhance the molecular level mixing. One of the ways of observing the turbulence effect on the non-premixed flame is to estimate the thickness of the flame. In the model scramjet, the non-premixed jet flame ignites due to the sudden temperature and pressure rises right behind the jet-induced bow-shock. Prior to the ignition, the fuel and air mix via fast diffusion and turbulence that can alter the fuel/air interface and mixture fraction

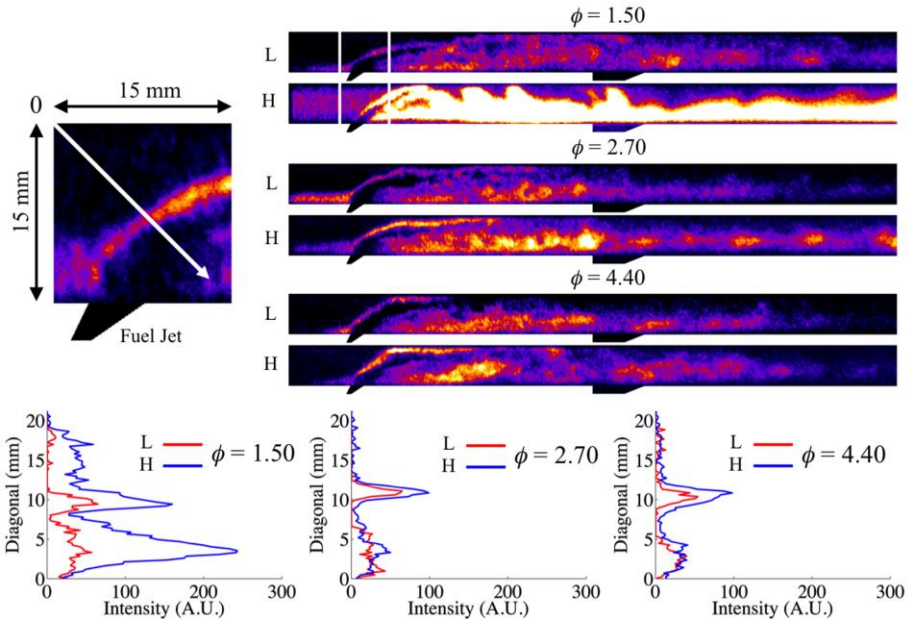

Figure 21. PLIF images and the LIF signal intensity profiles across the non-premixed flames in the Mach 4.5 freestream at P_0 = 0.65 bar, T_0 = 2,600 K and the overall equivalence ratio (ϕ) = 1.50, 2.70 and 4.40.

profile near the flame front; the turbulence can locally stretch the interface, increase the interfacial area, and/or steepening the local concentration gradient to enhancing the diffusive micro-mixing. In principle, the flame thickness of the non-premixed flame will be increased by the enhanced turbulence, and local combustion intensity will also be increased by improved mixing efficiency.

Figure 21 presents the LIF intensity profiles across the jet-induced bow-shock and the non-premixed jet flame on the windward side of the fuel jet at overall equivalence ratio (ϕ) = 1.50, 2.70 and 4.40, which were to estimate the non-premixed flame thickness. It was found that the non-premixed flame right behind the bow-shock is thicker and the flame is stronger (based on the comparison of the LIF intensity peak amplitudes) with the enhanced turbulence as expected. Moreover, the freestream turbulence also affects the long stretched flame originating from the fuel jet. It is noteworthy that the flame tail stretches far away from the bow-shock and therefore the flow near the long-stretched flame would be faster than that on the windward side of the fuel jet. Intuitively, one can conjecture the combustion reactions on the stretched flame that is almost parallel to the freestream will be rather mixing-controlled because the fuel/air mixing via diffusion would be relatively slow process considering the short flow residence time in the combustor of the high-speed flow.

To see the turbulence effect on the stretched mixing-controlled flame, two weak bow-shock conditions at ϕ = 0.25 and 0.50 are chosen to minimize the interferences from a strong bow-shock and the jet flame right behind it. The OH-PLIF images of the two fuel-lean cases in Fig. 22 confirm that the near-jet flames on the windward side are almost invisible though the stretched flame gets stronger as it gets far away from the fuel jet. When comparing the vertical LIF intensity profiles in low (L) and high (H) turbulence intensities at three different locations (indicated in Fig. 22), it is evident that the freestream

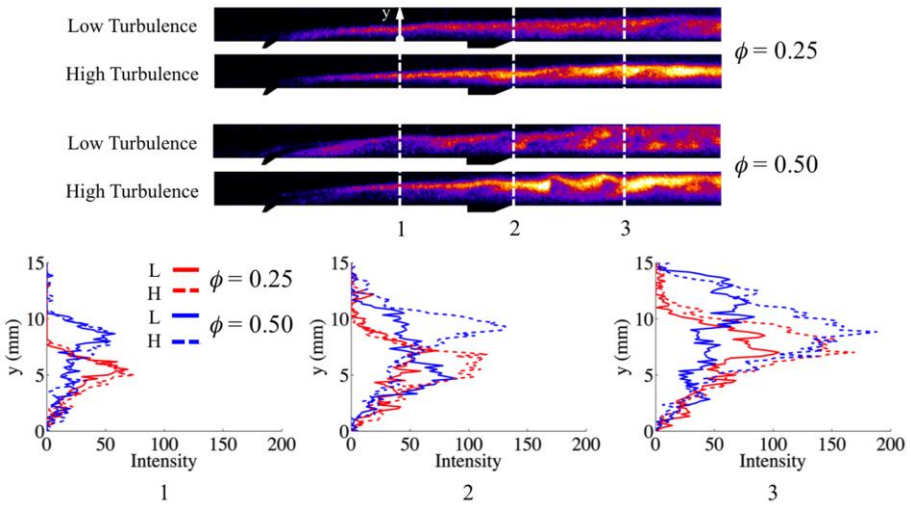

Figure 22. Vertical LIF signal intensity profiles at three different locations in Mach 4.5 freestream at P0 = 0.65 bar, T0 = 2,600 K, and overall equivalence ratio = 0.25 and 0.50.

turbulence significantly enhances the long-stretched non-premixed flame. This is again primarily due to the mixing enhancement on the fuel-air or jet-freestream interface by the freestream turbulence. Another interesting observation here is that the large-scale structure of the stretched flame is initially smooth and laminar-like shape while it is wrinkled in the further downstream region. It is previously reported that the transition of the laminar interface to wrinkled structures due to the flame instability could be promoted by the freestream turbulence while the trend is not clearly seen in this study. However, this is potentially a critical turbulence effect particularly when the stretched non-premixed flame is assisting the stabilization of a downstream partially-premixed flame.

Figure 23 shows a stretched non-premixed flame connected to an intense downstream partially-premixed flame when ϕ = 0.73. While the direct interaction between the stretched flame and the intense partially-premixed flame is not clear yet, it is evident that the upstream non-premixed flame helps the stabilization of the downstream flame via providing radicals and high temperature combustion products. The OH LIF signal profile in the direction of the scramjet flow presented in Fig. 23 (a) well describes the evolution of the flame that grows intenser along the flow direction. Four local fluorescence intensity peaks are indicated in the profile that correspond to the area 1 to 4 in the OH-PLIF image, which get significantly stronger. As the flame grows and the combustion reaction intensifies the accompanying heat release, downstream flow temperature rises to increase the flow viscosity and Kolmogorov scale while reducing characteristic reaction time scale, thus the Karlovitz number decreases. In other words, the scramjet flame that is spatially distributed in a wide area from the fuel jet to far downstream has variable and multiple time and length scales. In addition, it is evident that the characteristic reaction and flow

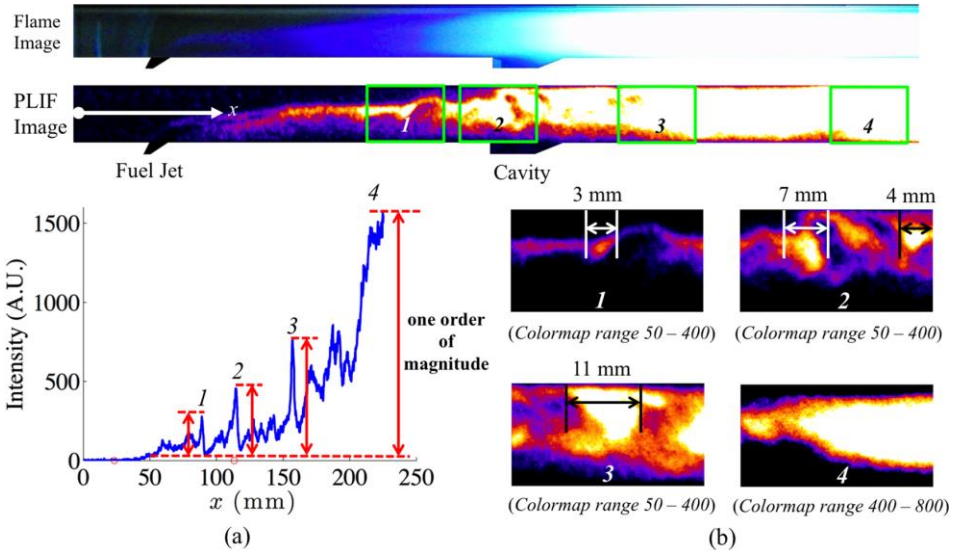

Figure 23. (a) A horizontal LIF signal intensity profile along the flow direction and (b) typical flame length scales seen in the OH-PLIF image with Mach 4.5 freestream (high turbulence) at P_0 = 0.65 bar, T_0 = 2,600 K, and the overall equivalence ratio ϕ = 0.73.

scales would be significantly affected by the flame and its dynamics. Again, the temporal/spatial flow scales determine the characteristics of the freestream turbulence, and the turbulence alters the flame dynamics in return, i.e., the freestream turbulence 'interacts' with the flame. According to a previously report, the chemical reaction time scale in scramjets varies from 10^{-6} s to 10^{-2} s and the flow time scales are on the order of 10^{-4} – 10^{-3} s in Mach 4.5 flows (absolute freestream velocity is approximately 2,000 m/s) that is comparable to the reaction time scale in this case. These scales are especially critical with premixed and partially-premixed flames because the ratio of the flow and reaction time scales ideally delineates the turbulent premixed flame regime such as wrinkled/corrugated flamelets and thin/broken reaction zones. When considering the reaction time scale and the freestream velocity (i.e., 1,000 – 2,000 m/s), the length scale of flame structure that is nearly parallel to the freestream could range from a few millimeters to meters in the direction of the freestream. As shown in Fig. 23, the characteristic length scale of the combustion localization zone observed in the OH-PLIF image varies from 3 mm to 11 mm and above at $\phi = 0.73$ along the flow direction prior to being merged to the intense and diffuse partially-premixed flame zone. Relatively small-scale flame structures (3 mm) are observed at the upstream location of area 1 where the combustion localization first appears. The typical flame length scale largely increases along the flow direction though multiple scales coexist (e.g., 7 mm and 4 mm in area 2 of Fig. 23 (b)) at the same time and location. In further downstream regions (area 3 and 4), larger flame structures (> 11 mm) appear and the PLIF signal saturates due to the intense partially-premixed flame. This trend is consistent with widely accepted theoretical approaches; decreasing Karlovitz number with increasing temperature would improve flame stability, intensify reactions and induce large-scale flame structures.

2 Summary

- The pulsed-arc-heated hypersonic wind tunnel (ACT-1) was built at ND.
- Turbulent non- and partially-premixed ethylene flame dynamics were investigated, and appropriate tunnel test conditions for the high-Reynolds combustion study were defined.
- A novel simultaneous fuel concentration and gas density measurement method was developed and successfully tested at high-enthalpy supersonic conditions (RC-19) at Wright Patterson Air Force Base.
- The ACT-1 freestream turbulence was manipulated using turbulence screens and a rapid flow contraction component providing uniform high-Reynolds flow fields.
- Investigations of freestream turbulence and its influences on scramjet flow structures were conducted.
- The turbulence influences on the supersonic combustion phenomena was systematically evaluated and reported.

1.

1. Report Type

Final Report

Primary Contact E-mail

Contact email if there is a problem with the report.

hyungrok@snu.ac.kr

Primary Contact Phone Number

Contact phone number if there is a problem with the report

82-10-7129-0656

Organization / Institution name

University of Notre Dame/Seoul National University

Grant/Contract Title

The full title of the funded effort.

EXPERIMENTAL INVESTIGATION OF TURBULENT FLAMES IN HYPERSONIC FLOWS

Grant/Contract Number

AFOSR assigned control number. It must begin with "FA9550" or "F49620" or "FA2386".

FA9550-12-1-0161

Principal Investigator Name

The full name of the principal investigator on the grant or contract.

Hyungrok Do

Program Manager

The AFOSR Program Manager currently assigned to the award

Chiping Li

Reporting Period Start Date

04/01/2012

Reporting Period End Date

06/30/2015

Abstract

Work during the three-year project timeframe has been focused on 1-1) completing the construction of an arc-heated hypersonic combustion test rig (ACT-1) at the University of Notre Dame (ND), 1-2) characterizing turbulent flame dynamics under various supersonic and hypersonic freestream conditions (Mach 4.5, 6 and 9), and 1-3) developing tools for quantitative turbulent flow measurement methods (in collaboration with Dr. Campbell D. Carter of AFRL) including a new laser diagnostics technique for simultaneous fuel concentration and gas density measurements in supersonic combustors, and 1-4) controlling/quantifying freestream turbulence and evaluating its influences on the turbulent flame dynamics in the high-Reynolds scramjet flows. The new arc-heated hypersonic facility construction was completed at ND in the second project year, which has been fully operational afterwards for the supersonic/hypersonic turbulent combustion study. The studies on the supersonic flame dynamics were successfully conducted revealing non-premixed/partially-premixed characteristics of the ethylene flames in the model scramjet installed in the hypersonic facility. The experimental results also confirmed the critical effects of the freestream turbulence on the flame dynamics both for partially- and non-premixed configurations. In addition, a new laser diagnostics tool specialized for the high-enthalpy scramjet study has been developed and used in collaboration with AFRL at Wright Patterson Air Force Base. This technique was proven to be working perfectly under the harsh flow conditions of high-speed (Ma > 4.5) and high-temperature (>

1,500K) that limit quantitative measurements.

Distribution Statement

This is block 12 on the SF298 form.

Distribution A - Approved for Public Release

Explanation for Distribution Statement

If this is not approved for public release, please provide a short explanation. E.g., contains proprietary information.

SF298 Form

Please attach your SF298 form. A blank SF298 can be found here. Please do not password protect or secure the PDF The maximum file size for an SF298 is 50MB.

AFD-070820-035_Hyungrok Do 2.pdf

Upload the Report Document. File must be a PDF. Please do not password protect or secure the PDF . The maximum file size for the Report Document is 50MB.

Final report Hyungrok Do.pdf

Upload a Report Document, if any. The maximum file size for the Report Document is 50MB.

Archival Publications (published) during reporting period:

1. B. McGann, C. D. Carter, T. Ombrello, and H. Do, 2105 “Direct Spectrum Matching of Laser Induced Breakdown for Hydrocarbon Fuel Concentration and Gas Density Measurements in Compressible Reacting Flows,” Combustion and Flame, Accepted for Publication.
2. H. Do, C. D. Carter, Q. Liu, T. Ombrello, S. Hammack, T. Lee and K. –Y. Hsu, 2015, “Simultaneous density and fuel concentration measurement in a supersonic combustor using laser induced breakdown,” Proceedings of Combustion Institute 35 (2): 2155–2162.
3. Q. Liu, A. Passaro, D. Baccarella, and H. Do, 2014, “Ethylene Flame Dynamics and Inlet Unstart in a Model Scramjet,” Journal of Propulsion and Power 30 (6): 1577-1585.
4. H. Do and Carter, C. D., 2013, “Hydrocarbon fuel concentration measurement in reacting flows using short-gated emission spectra of laser induced plasma,” Combustion and Flame, 160: 601–609.

Changes in research objectives (if any):

Change in AFOSR Program Manager, if any:

Extensions granted or milestones slipped, if any:

AFOSR LRIR Number

LRIR Title

Reporting Period

Laboratory Task Manager

Program Officer

Research Objectives

Technical Summary

Funding Summary by Cost Category (by FY, $K)

	Starting FY	FY+1	FY+2
Salary			
Equipment/Facilities			
Supplies			
Total			

Report Document

Report Document - Text Analysis

Report Document - Text Analysis

Appendix Documents

2. Thank You

E-mail user

Aug 31, 2015 12:23:32 Success: Email Sent to: hyungrok@snu.ac.kr